CFD INVESTIGATION OF AIRFLOW AROUND OBJECTS WITH DIFFERENT SHAPES

Jane W Z Lu, Isaac Y F Lun, Joseph C Lam
Department of Building & Construction, City University of Hong Kong,
83 Tat Chee Avenue, Kowloon Tong, Kowloon, Hong Kong

ABSTRACT

A two-dimensional numerical simulation of airflow around bluff bodies is presented in this study. The two turbulence models, i.e., standard k-ε model and RNG k-ε model, are employed to predict the flowfield and wind effects on bluff bodies. The results of the study highlight and compare the discrepancies between these two turbulence models in capturing the flow structure around bluff bodies, particularly in the vicinity of surfaces.

INTRODUCTION

Due to the rapid population expansion, it is almost a definite tendency that high skyscrapers can be found in all metropolitan cities, especially in Asia. Newly constructed high-rise structures tend to be the artistic creation in modern architectural fashion rather than the actual need for the society. The shapes of these structures can be cylindrical, square column or arbitrary. The feature view of such structures surely gives good impression to the public; however, subsequent building problems such as wind related may be incurred.

The airflow around bluff body located in atmospheric environment is extremely complex and fully turbulent as well as its pattern can be very different from one to another. These airflow patterns are important factors in predicting wind effects on building and its surroundings. In engineering discipline it is possible to model some of the wind effects on buildings by using the conventional boundary layer wind tunnels. The scaling ratios involved together with the effects of surface roughness mean that caution has to be applied in the interpretation of such data. The lurking risk by using such conventional method has been recognized to certain extent. In recent years the rapid development of computer technology has stimulated the growth of computational method to investigate large-scale and complex problems. Over the last decade, Computational Wind Engineering (CWE) as a branch of Computational Fluid Dynamics (CFD) has been developed rapidly to evaluate the interaction between wind and building numerically. It offers an alternative new approach for practical applications both in engineering and research.

A wide variety of numerical studies have been reported in modelling the airflow around buildings[1-16]. Numerical prediction by means of Large Eddy Simulation (LES) and k-ε model are commonly adopted to simulate wind flows around bluff bodies in wind engineering. LES models can be applied to large scale turbulent flows and it can produce better predictions of the entire flow pattern encompassed a bluff body[1] than the standard k-ε model does. It also provides higher accuracy than other turbulence models but it requires much more computational capacity[2]. This type of model needs much finer grids than what is possible at present for larger simulation and it does not appear in literature that a reliable method for taking surface roughness into account without actually meshing it. The k-ε model has a good reputation for its reliability of simulation and appears to be most promising for present practical applications in wind engineering[3]. A number of industrial and wind engineering applications of the two equation k-e turbulence model have been applied and examined[4,5,6]. In wind engineering application, the k-ε model is the most reliable approach with a reasonable accuracy and computational cost in predicting wind flows around bluff bodies[7]. Thus the k-ε turbulence model and its revised form, RNG k-ε, are used in the current work due to its simplicity and cost effectiveness.

The study reported in this paper is to perform numerical simulation of the airflow around bluff bodies with different geometry. The aims are to provide information to enhance the understanding of the flow phenomena, the wind effects on bluff body surfaces and the influence of turbulence models on simulating flowfields.

MATHEMATICAL DESCRIPTION

Computational Fluid Dynamics method is employed in the numerical simulations. The Eulerian mathematical model is used to simulate the continuous fluid flow. The standard k-ε and RNG k-ε turbulence models are applied in the study to take account of turbulence influence on both airflow field and particle movement. The equation sets are listed below:

Table 1 Source terms in the conservation equation

Equation	Φ_i	Γ_{ϕ_i}	S_{ϕ_i}
Continuity	1	0	0
U_i momentum	U_i	$\mu+\mu_t$	$-\frac{\partial}{\partial x_i}\left(P+\frac{2}{3}\rho k\right)+\frac{\partial}{\partial x_i}\left[(\mu+\mu_t)\left(\frac{\partial U_i}{\partial x_j}+\frac{\partial U_j}{\partial x_i}\right)\right]+F_B$
Kinetic energy	k	$\mu+\frac{\mu_t}{\sigma_k}$	$P+G-\rho\varepsilon$
Dissipation rate	ε	$\mu+\frac{\mu_t}{\sigma_\varepsilon}$	$C_1\frac{\varepsilon}{k}(P+C_3\,max(G,0))-C_2\rho\frac{\varepsilon^2}{k}$

a. General governing equation for continuous fluid flow:

$$\frac{\partial(\rho\phi_i)}{\partial t}+\mathrm{div}(\rho U\phi_i)-\mathrm{div}(\Gamma_{\phi_i}\nabla\phi_i)=S_{\phi_i} \qquad (1)$$

The details can be seen in Table 1.

The constants appeared in Table 1 are defined as follows:

$$\mu_t=C_\mu\rho\frac{k^2}{\varepsilon} \qquad (2)$$

For RNG k-ε: C_1 becomes C_1-C_{1RNG}; where

$$C_{1RNG}=\frac{\eta\left(1-\frac{\eta}{\eta_o}\right)}{(1+\beta\eta^3)} \qquad (3)$$

$$\eta=\frac{P^{0.5}}{\mu_t}\frac{k}{\varepsilon} \qquad (4)$$

The constants in above models are assigned the following values, which were recommended by the references[18]:

k-ε: C_1=1.44, C_2=1.92, C_3=0, C_μ=0.09, $\sigma_k=1.0, \sigma_\varepsilon=1.3$

RNG k-ε: C_1=1.42, C_2=1.68, C_3=0, C_μ=0.085, σ_k=0.085, σ_ε=0.419, β=0.015, η_o=4.38

The numerical approach regards flow medium as a continuous fluid, solves the whole set of equations for the continuum at all control volumes and obtains the values of fluid velocity, pressure, turbulence parameters, etc., over the whole flow field.

b. Boundary conditions for the airflow

The boundary conditions, specified for the airflow, in this study, are defined as follows:

- All variables at the upstream of the flow domain are set according to the principles of Dirichlet boundary condition. A uniform velocity profile is specified at inlet side ($R_e\approx10^5$). The quantities k and ε at the inlet are based on the mean flow characteristics at the inlet section, i.e., the inlet velocities;
- A non-slip condition at the solid wall is applied to the velocities. The wall function is employed to describe the turbulent properties in near wall regions;
- Free boundary conditions are applied at the outsides of flow domain to satisfy the mass conservation.

c. Boundary conditions for turbulent flow

Due to the damping effect of the wall surfaces, the transport equations do not accurately represent the turbulence in the near-wall region[17-18]. Turbulent parameters vary rapidly in the near-wall region. The alternative is to extend the Couette flow analysis and apply algebraic relations, the so-called logarithmic laws or wall function concepts, to the near-wall region. The main idea of wall function approximation is based on this: the flow in near wall region can be divided into three sublayers, i.e., laminar sub-layer, buffer zone, and fully turbulent layer[17-18]. Although flow in near-wall region comprises three zones, the wall function approach assumes that the flow in near-wall region can be generally divided into laminar region and turbulent region. The scalar variables, i.e., scalar velocity u^+, scalar co-ordinate y^+, have been defined in wall function approach:

Scalar velocity $$u^+=\frac{u\left(C_\mu^{1/4}k^{1/2}\right)}{\tau_w/\rho} \qquad (5)$$

Scalar co-ordinate $$y^+=\frac{y\left(C_\mu^{1/4}k^{1/2}\right)}{\nu} \qquad (6)$$

In the simulations, let y_o^+ denotes the junction point of laminar and turbulent region (for smooth wall surface, y_o^+=11.6), then the wall function can be expressed as below[13. 15]:

$$u^+ = \begin{cases} y^+ & y^+ < y_o^+ \\ \frac{1}{\kappa}\ln\left(Ey^+\right) & y^+ > y_o^+ \end{cases} \quad (7)$$

$$\varepsilon = \frac{C_\mu^{3/4} k^{3/2}}{\kappa y} \quad (8)$$

RESULTS ANALYSIS

Two shapes of bluff body, square and circle, are considered in the current study. The characteristic dimensions, D, of the square is 35m and the diameter of the circle is specified as 35m. The computational flow domains of two cases are both identical. The upstream and downstream lengths are 16D and 38D respectively. The control cells of the models is 22252 with denser region closely allocated around the object. Figure 1 shows the computational meshes of the two cases; (a) is the square model and (b) is the circle model. Two types of turbulence model, namely standard k-ε (S) and revised k-ε (RNG), are used in the present work. The turbulent kinetic energy, pressure coefficient and u-velocity of the numerical predictions are analyzed at difference locations along the streamwise direction of the flow domain. Figure 2 shows the geometrical flow domain and the positions in which k, Cp and Ux are analyzed. The horizontal velocity Uo=3m/s, turbulent kinetic energy k=0.9062 and turbulent dissipation ε=7.682e-3 are set at the inlet. Figure 3 shows the turbulent kinetic energy, k, at different sections of the model. Figure 3 (a, b, c) shows that the standard type of k-ε predictions has distinctive differences with the RNG model. When the flow approaches closer to the object, more steeply slopes are observed. These slopes indicated that the k values grow due to the increase of velocity. At the windward corners of the square the k values start dropping until the velocity reaches the stagnation point. It is shown evidently in figure 3b and 3c the standard k-ε type can only model the general form of flow around an object, in nearest the object surface RNG type is more appropriate. Figure 3 (d, e, f) depicts the k around circle. Results are relatively similar as those obtained in figure 3(a, b, c), except at the position 2 & 3 by the RNG model. This could be due to the influence of the flow separation on the incoming flow around the square corners at windward side, whilst separation occurred in the circle case has no effect on the incoming flow.

The pressure distributions at different sections and along the object surface of the models are expressed in figures 4 & 5 respectively. Square pressure coefficients obtained, in figure 4a, by the standard k-ε model are overpredicted than those by RNG model. Different pressure drops produced by two models are depicted in figure 4b. A bimodal pressure coefficient predicted by RNG model is found at position 2 whilst the standard model shows the Cp distributing evenly. Moving proximity to the bluff body, in figure 4c, an indication is highlighted that standard k-ε model may not perform well than the RNG model. Figure 4d, 4e and 4f show the pressure results of the circle case. Figure 5 shows the pressure distribution along the circle surface. Two different pressure coefficient curves are generated by the standard and RNG models, after 45^0, no evident difference in Cp can be observed. The Cp decreases gradually and recovers to certain extent at around 90^0, separation occurs until 135^0.

The velocity vectors of square and circle are presented in figure 6. In both plots, vortexes can be seen at the rear end of the objects. A patch of small arrows situated at the frontal corners of the square indicating where the separation regions are generating. The sizes of vortex behind the circle are small due to the high velocity clip off from the circle producing a push to them. Horizontal velocities at different position along the computational flow domain are performed in figure 7. The velocities distribute fairly reasonably for the square model (figure 7a & 7b) except at the vicinity of the front and rear faces (figure 7c). The curves of the k-ε model in this figure do not capture accurately at the front corners, while the RNG model performs distinctively. The horizontal velocities of the circle model are illustrated in figure 7d, 7e and 7f. There are no noticeable discrepancy observed in the case.

CONCLUSIONS

Numerical predictions of airflow around bluff bodies by two k-ε based turbulence models are carried out and reported here. The distributions of turbulent kinetic energy, pressure coefficient and horizontal velocity at different position along the flow domain are presented and examined. The results obtained from the study show that the revised RNG k-ε model has better capability in simulating flowfield close to object with sudden changes in geometry. Whilst the standard k-ε model can predict flow pattern to certain accuracy but fail to produce the interaction between the turbulent structure and the bluff body profile. However, applying these two turbulence models to smooth surface body, no significant discrepancy in results is observed. The experimental study is required in future to validate the numerical analyses.

REFERENCES

1. Murakami, S. and Mochida, A., ' Three-dimensional numerical simulation of air flow around a cubic model by means of large eddy

simulation ‘, J. Wind Eng. Ind. Aerodyn., Vol. 25, pp. 291-305, 1987.
2. Murakami, S., ‘ Comparison of various turbulence models applied to a bluff body ‘, J. Wind Eng. Ind. Aerodyn., Vol. 46 & 47, pp. 21-36, 1993.
3. Murakami, S. and Mochida, A., ‘ 3-d numerical simulation of airflow around a cubic model by means of the k-ε model ‘, J. Wind Eng. Ind. Aerodyn., Vol. 31, pp. 283-303, 1988.
4. Paterson, D.A. and Apelt, C.J., ‘ Simulation of wind flows around three-dimensional buildings ‘, Building and Environment, Vol. 24, No.1, pp. 39-50, 1989.
5. Paterson, D.A. and Papenfuss, A.T., ‘Computation of wind flows around two tall buildings ‘, J. Wind Eng. Ind. Aerodyn., Vol. 50, pp. 69-74, 1993.
6. Murakami, S., ‘ Overview of turbulence models applied in CWE-1997 ‘, Proceedings of 2nd European & African Conference on Wind Engineering, Vol. 2, pp. 3-24, Genova, Italy, 1997.
7. Paterson, D.A., ‘ Computation of wind flows over three-dimensional buildings ‘, PhD Thesis, The University of Queensland, 1986.
8. Jones J & Whittle G E, ' Computational Fluid Dynamics for building air flow prediction - current status and capabilities ', Journal of Building and Environment, Vol. 27(3), 321~338, 1992.
9. Ferziger, J., ‘ Simulation of complex turbulent flows: recent advances and prospects in wind engineering ‘, J. Wind Eng. Ind. Aerodyn., Vol. 46 & 47, pp. 195-212, 1993.
10. Kawamoto, S. and Tanahashi, T., ‘ High-speed GSMAC-FEM for wind engineering ‘, Computer Methods in Applied Mechanics and Engineering, 112, pp. 219-226, 1994.
11. Yu, D. H. and Kareem, A., ‘ Simulation of probabilistic flow field around two-dimensional rectangular prisms utilizing LES ‘, IWEF Workshop on CFD for Prediction of Wind Loading on Buildings and Structures, September 9, 1995.
12. Lu, W Z, Lun, Y F & Jeary, A P, ' CFD simulation of airflow around a bluff structure - Central Plaza, Part II', Department of Building & Construction, City University of Hong Kong, Report No. BC-SDRC/97/27, 1997.
13. Lu, W Z, Lun, Y F & Jeary, A P, ' CFD simulation of airflow around a bluff structure - Central Plaza, Part I', Department of Building & Construction, City University of Hong Kong, Report No. BC-SDRC/97/26, 1997.
14. Lu, W Z, Lun, Y F & Jeary, A P, ' CFD simulation of airflow around a high-rise building - Central Plaza Tower in Hong Kong Island ', Department of Building & Construction, City University of Hong Kong, Report No. BC-SDRC/97/23, 1997.
15. Lu, W Z, Lun, Y F & Jeary, A P, ' CFD simulation of airflow around high-rise building - Bank of China Tower ', Department of Building & Construction, City University of Hong Kong, Report No. BC-SDRC/97/15, 1997.
16. Lu, W Z, Lun, Y F & Jeary, A P, ' CFD simulation of airflow pattern around high-rise building ', Department of Building & Construction, City University of Hong Kong, Report No. BC-SDRC/97/10, 1997.
17. Lu W, Howarth A T, Adam, N & Riffat, S B, ' Modelling and Measurement of Airflow and aerosol particle distribution in a ventilated two-zone chamber ', Building & Environment, Vol. 31(5), 417~423, 1996.
18. Launder B E & Spalding D B, ' The numerical computation of turbulent flows ', Computational Methods in Applied Mechanics & Engineering, Vol. 3, 269~289, 1974.

NOMENCLATURE

F_B	body force exerted on fluid (N/m^3)
P	turbulent generation term
k	kinetic energy of turbulence ($½u_iu_i$)
S_{ϕ_i}	source term
U_i	velocity in i-direction (m/s)
u^+	scaled velocity parallel to wall
w	wodth (m)
y^+	scaled distance to wall surface
ϕ_i	dependent variable of general equation
Γ_{ϕ_i}	diffusive coefficient in general equation
ε	turbulent energy dissipation rate(m^2/s^3)
κ	von Carmen constant, κ=0.4~0.44
μ	dynamic viscosity of fluid (kg/m·s)
μ_t	turbulent dynamic viscosity of fluid (kg/m·s)
ρ	density of fluid (kg/m^3)
σ_k	Prandtl number of k
σ_t	turbulent Prandtl (Schmidt) number
σ_ε	Prandtl number of ε

Square Circle

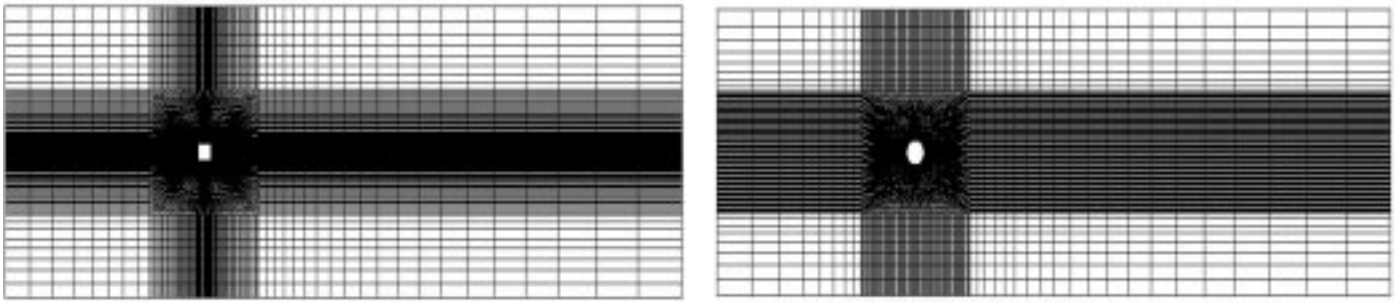

(a) (b)

Figure 1 Computational mesh of models used

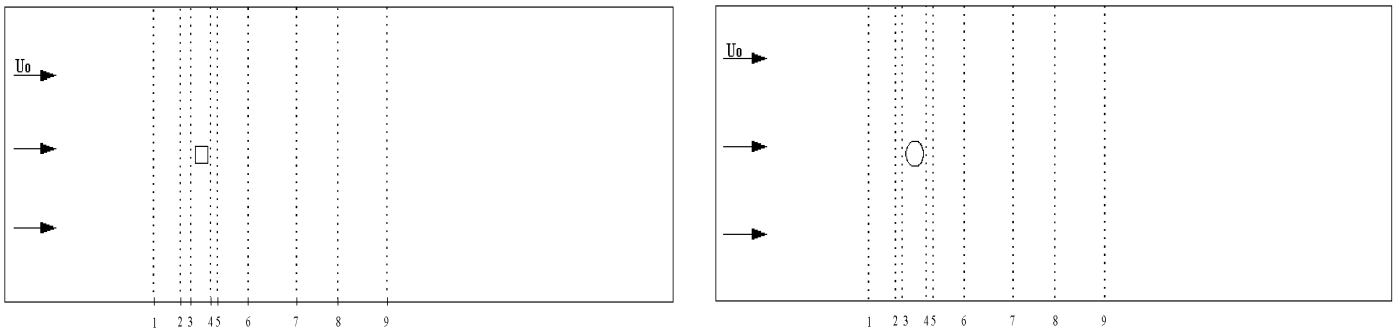

Figure 2 Geometrical outlines and analysed positions of test cases

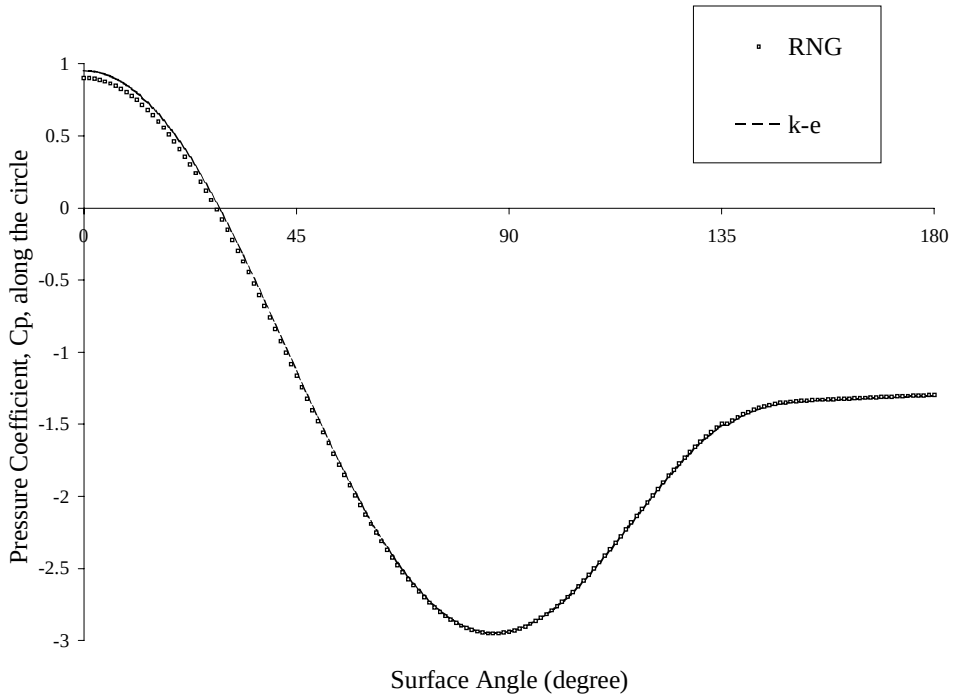

Figure 5 Pressure loading along the circle surface by k-ε and RNG (k-ε)

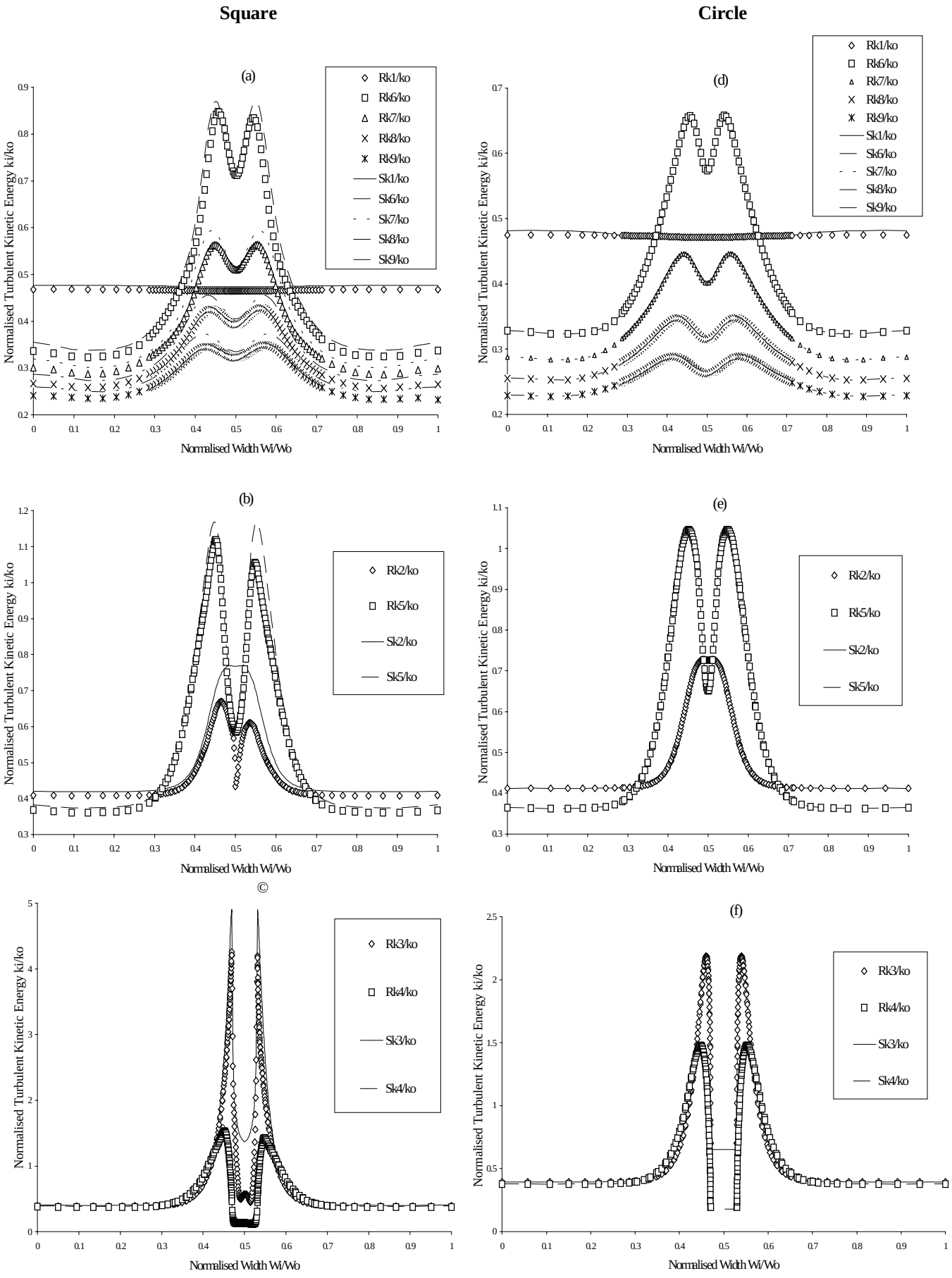

Figure 3 Distributions of turbulence kinetic energy at different sections between two models (a, b, c for square; d, e, f for circle; Rk — the RNG model, Sk — the standard k-ε model. The numbers referred to figure 2)

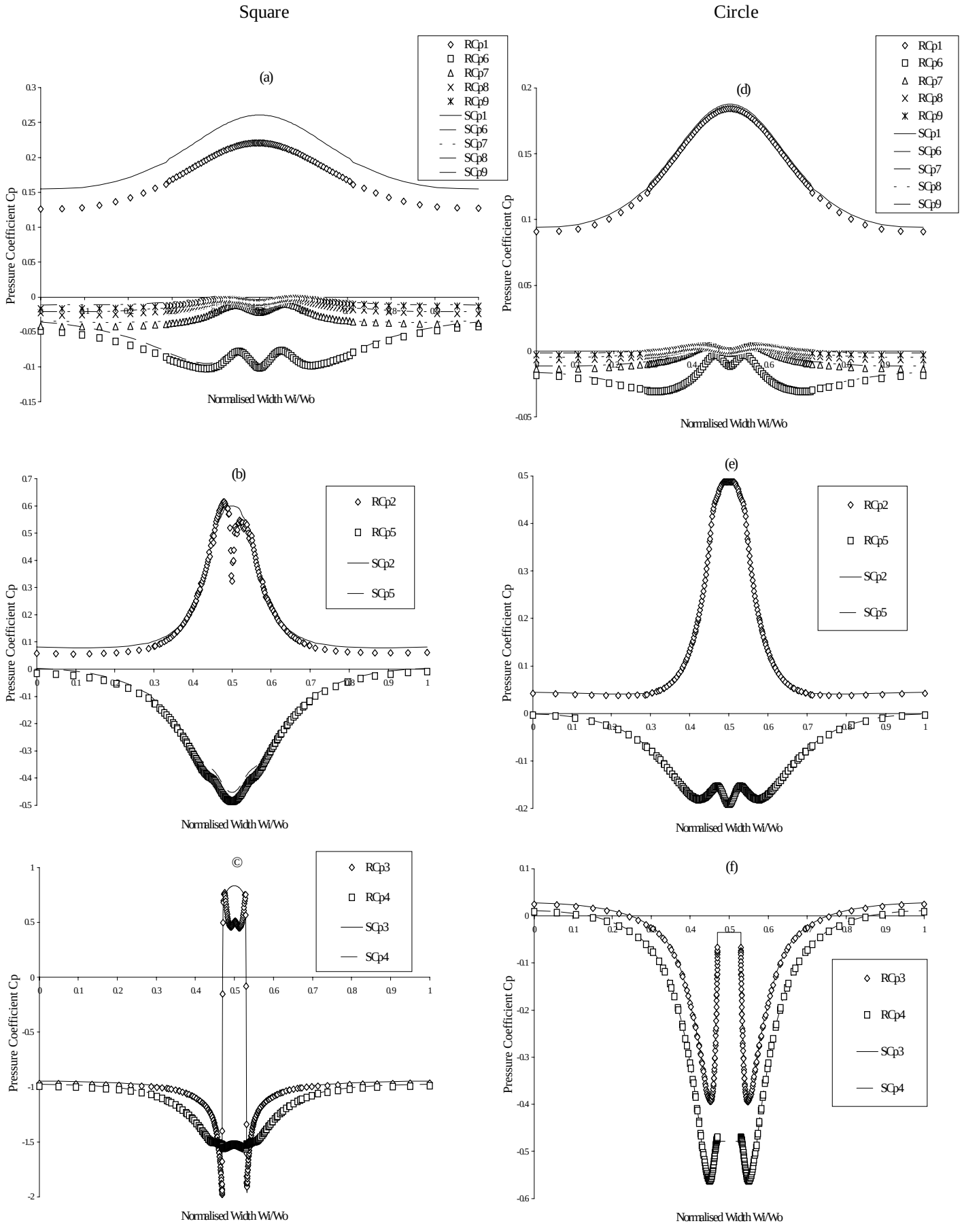

Figure 4. Pressure Coefficient produced by k-ε and RNG (k-ε) at different sections (a, b, c for square; d, e, f for circle; RCp — the RNG model, SCp — the standard k-ε case. The numbers referred to figure 2)

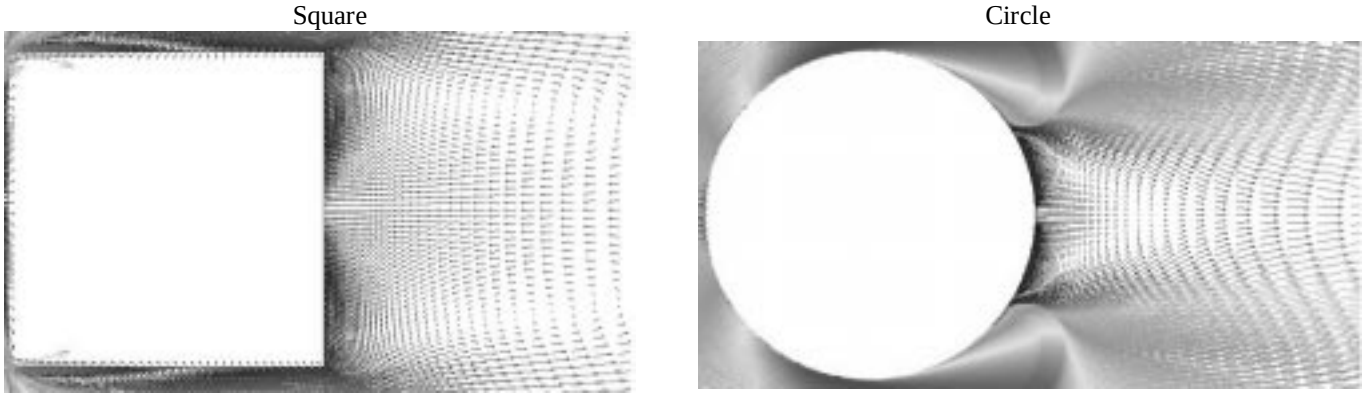

Figure 6 Airflow pattern at the leeward sides of bluff bodies for the RNG k-ε case

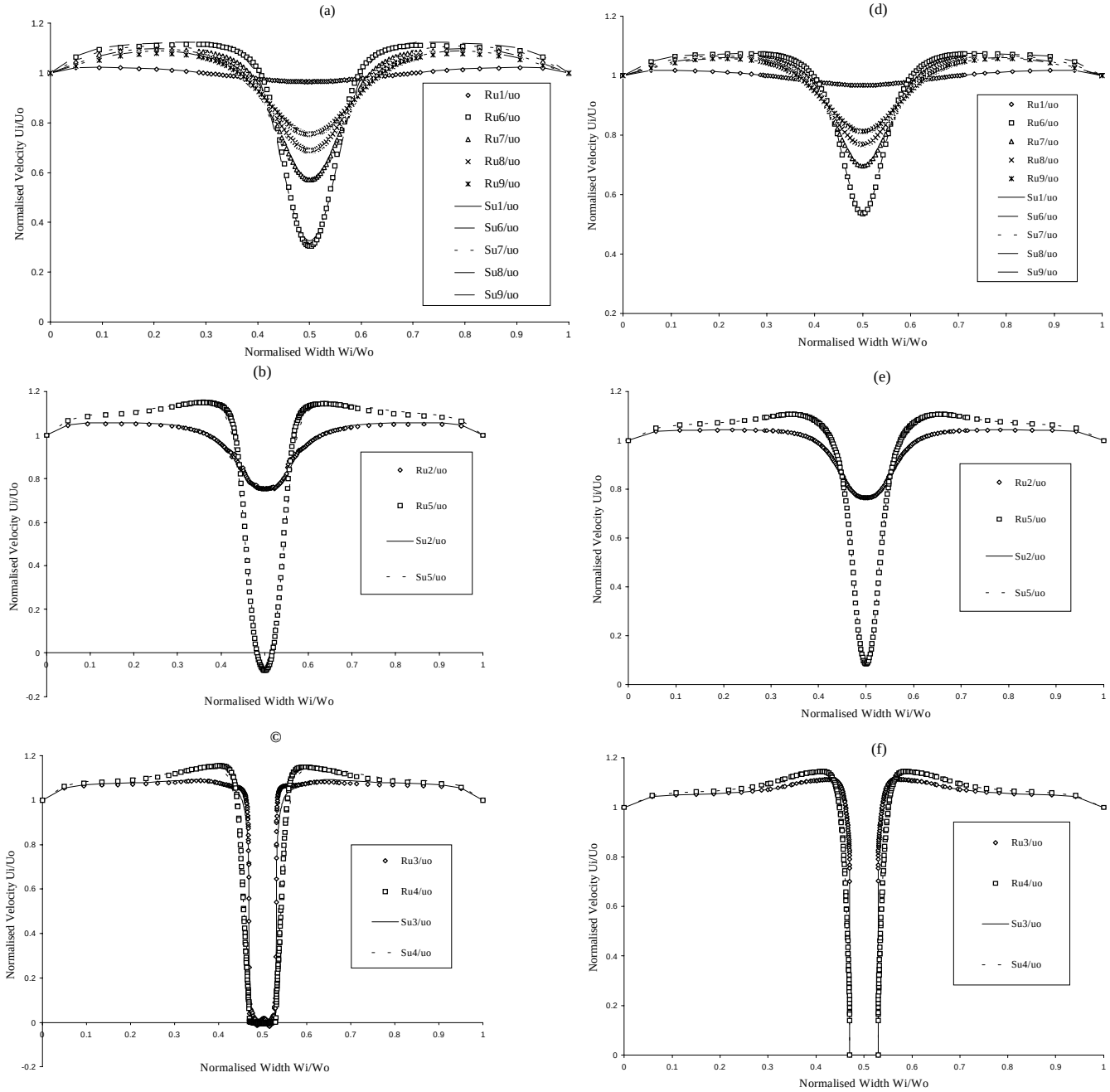

Figure 7 Comparison of horizontal velocity distributions at different sections between two models (a, b, c for square; d, e, f for circle; Ru — the RNG model, Su — the standard k-ε model. The numbers referred to figure 2)